Supplementary Material

Nano-Graphene Oxide for Cellular Imaging and Drug Delivery

Xiaoming Sun, Zhuang Liu, Kevin Welsher, Joshua Tucker Robinson, Andrew Goodwin, Sasa Zaric, and Hongjie Dai*

Department of Chemistry and Laboratory for Advanced Materials, Stanford University, Stanford, CA 94305, USA

Supporting information to DOI 10.1007/s12274-008-8021-8

Part I. Additional experimental details

Method used to determine the weight ratio of graphitic carbon (GC) in expandable graphite. As illustrated in the Method section, pegylated nano-graphene oxide (NGO–PEG) was made from expandable graphite. Functional groups were added by oxidization, and PEG molecules were grafted on by means of *N*-(3-dimethylaminopropyl-*N*′-ethylcarbodiimide) hydrochloride (EDC). In order to determine the graphitic carbon mass ratio in the final product, we used the following method to determine the graphitic carbon ratio in the starting expandable graphite:

Raw expandable graphite (Graftech Inc.) (20–30 mg) was weighed and then heated at 900 °C for 1 h under argon protection to fully remove intercalated acid molecules. Upon cooling to room temperature, the graphite was weighed again to determine the graphitic carbon mass. The mass loss in this step was ~25%. According to information provided by the company (see link: http://www.graftechaet.com/Technical-Documents/Technical-Bullitin/TB226-GG-GG-DESC.pdf), the onset of exfoliation temperature was 160 °C. Therefore, heating at 900 °C for 1 h should be sufficient to drive off any gaseous species from the expandable graphite. The resulting product contains ~75% of the original carbon mass.

Methods of UV-vis-NIR absorption and PLE spectroscopy measurements on solutions of GO, GO–COOH and NGO–PEG with the same GC concentration. Since ~15% of carbon was lost in the grinding and filtration step and the carbon mass from the starting expandable graphite is ~75%, the graphitic carbon in the final product was calculated to be 64% (75% × 85%). That is, 0.64 g of carbon is used for the final carbon mass calculation when 1 g of expandable graphite was used as the starting material. This is based on the assumption that the graphitic carbon loss during oxidization and pegylation can be ignored.

To obtain optical spectra of GO and NGO–PEG solutions of known concentration, care was taken to minimize material loss in all steps, including oxidization, activation, and pegylation. The filtrate and centrifuge supernatant obtained in purification cycles were collected and measured by absorption spectrometry. We concluded that the graphitic carbon loss during the reaction was < 2% by comparing the absorbance and volumes at 500 nm. Final products (GO, GO–COOH and GO–6PEG) were diluted with DI water to make solutions with identical graphitic carbon mass concentration. These solutions were then used to obtain absorption spectra (Fig. 2(a)) and photoluminescence excitation spectra (Fig. 2, (c) and (d)).

Atomic force microscopy (AFM). Si wafers with natural SiO_2 surfaces were treated with 0.6% APTES (3-aminopropyltriethoxysilane) for 5 min. GO or NGO–PEG was deposited by soaking the substrate in a diluted solution for ~2 min. The substrate was rinsed with water, blow-dried with air, and imaged by tapping mode AFM.

AFM tip size correction. This correction was important since the particle size of NGO–PEG was mostly less than 20 nm. We used a single-walled

carbon nanotube (SWNT) sample for tip correction. We measured the apparent width (W) and height (H) of SWNTs by regular Si tips. The tip size can be calculated from the formula:

$$\text{Tip size} = \frac{1}{2}(W-H)$$

This was used to correct for the graphene sheet size measured:

True sheet size = Measured size – 2 × (tip size)

UV-vis-NIR absorption spectroscopy. Absorbance measurements in the UV-vis-NIR range were carried out using a Cary 6000i spectrophotometer. Graphene and graphene oxide solutions were measured in a 1 mm path quartz cuvette. We used a cuvette filled with water in a double beam geometry to subtract background due to water absorption.

Photoluminescence excitation/emission spectroscopy. Photoluminescence excitation (PLE) measurements were performed utilizing a home-built setup. A short arc lamp (Osram XBO 75W/2 OFR 75W Xenon lamp installed into an Oriel 66907 Arc Lamp Source) and a monochromator (Oriel 7400 Cornerstone 130 monochromator) were used to supply excitation light in the 550–840 nm range in 10 nm steps. The excitation light was focused onto a sample placed in a 1 mm path quartz cuvette. The room temperature sample photoluminescence was collected in a transmission geometry and the PL spectrum was recorded using a second monochromator (Acton SpectraPro 2300i) and a liquid nitrogen-cooled InGaAs array detector (Princeton Instruments OMA V 1024-2.2 LN) in the 900–1500 nm range. As-obtained PL spectra were scaled by the measured excitation power (measured using an Oriel 71580 calibrated Si photodiode) before obtaining a PLE spectrum by interpolating the 30 measured PL spectra. The bandpass used for emission and excitation was 15 nm.

Antibody conjugation. Thiolated antibody (Rituxan was a gift of Drs. Alice Fan and Dean Felsher) was conjugated to the amine groups on NGO–PEG via a sulfosuccinimidyl 4-*N*-maleimidomethyl cyclohexane-1-carboxylate (Sulfo-SMCC) linker. The thiolation was done by mixing antibody (10 mg/mL) with Traut's reagent (Pierce) at a 1:10 molar ratio in phosphate buffered saline (PBS) in the presence of 20 mmol/L EDTA (final pH ~8) for 2 h. Unreacted Traut's reagent was removed by filtration through a 100 kDa filter. The thiolated antibody was used immediately in the subsequent conjugation. NGO–PEG at a concentration of ~0.2 mg/mL was reacted with 1 mmol/L Sulfo-SMCC (Pierce) for 2 h in PBS at pH 7.4. After thorough removal of excess Sulfo-SMCC by filtration through a 100 kDa filter, the NGO–PEG solution was mixed with thiolated antibody in PBS in the presence of 2 mmol/L EDTA. In the reaction buffer, the final NGO-PEG concentration was ~0.2 mg/mL, while that of antibody was 10 μmol/L. The reaction was allowed to proceed overnight at 4 °C, affording the NGO–PEG antibody conjugate. This conjugate was used directly without further treatment.

Part II. Supplementary materials

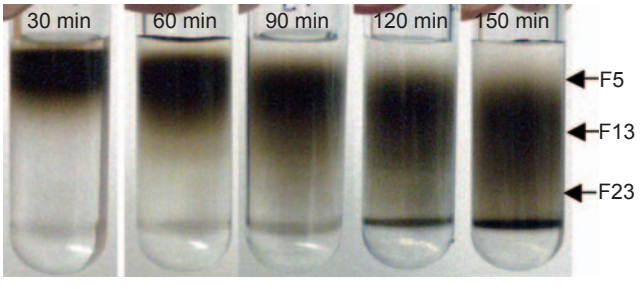

(a)

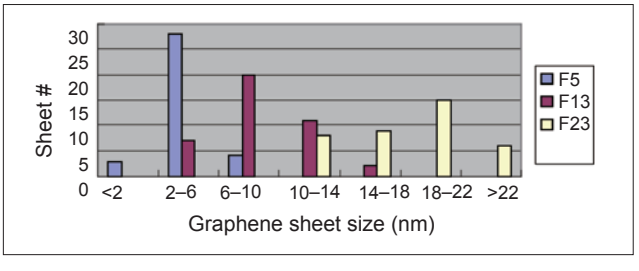

(b)

Figure S-1 Separation of NGO–PEG: (a) Photographs of ultracentrifuge tubes containing density gradients after ultracentrifuge at $3\times10^5 g$ for different time points from 30 min to 150 min as labeled; (b) Histogram of graphene sheet lateral size after separation.

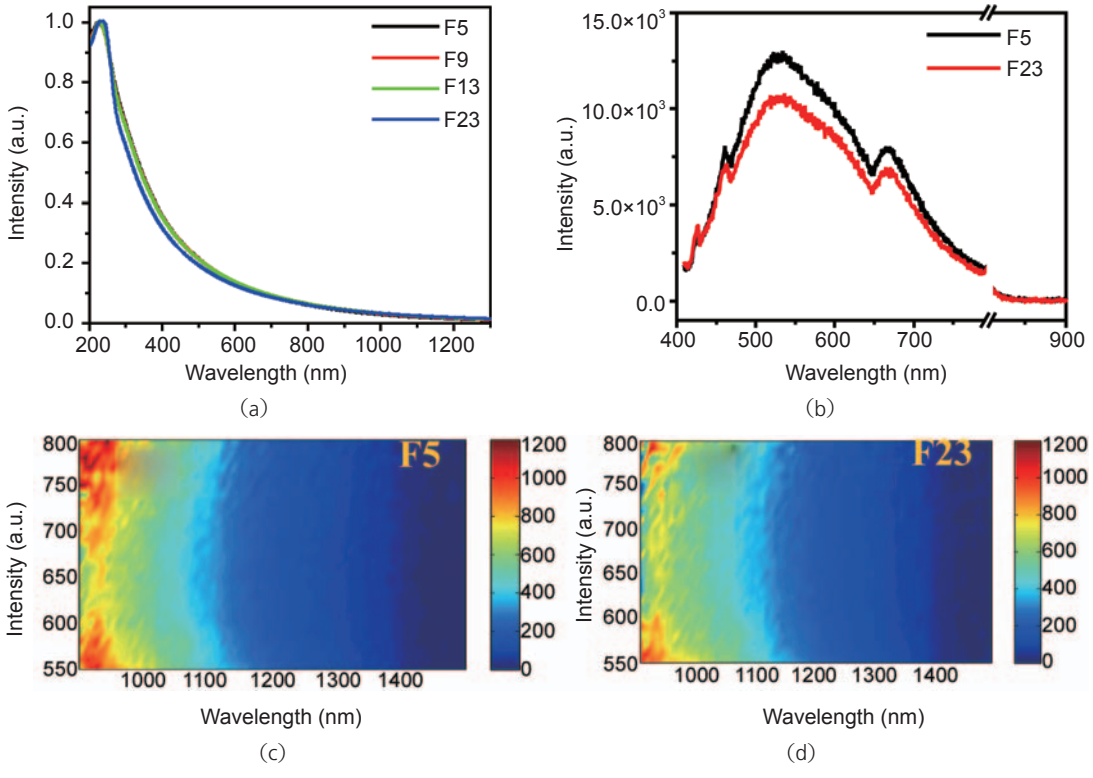

Figure S-2 Comparison of optical properties of graphene sheet fractions after separation: (a) Absorbance spectra of fractions with different sizes. F5, F9, F13, and F23 were as labeled in Fig. S-1 (a); (b) Photoluminescence spectra of F5 and F23 in the visible range with 400 nm excitation; (c), (d) Photoluminescence excitation spectra of F5 and F23 with excitation at 550–800 nm. All the photoluminescence was normalized to absorbance spectra

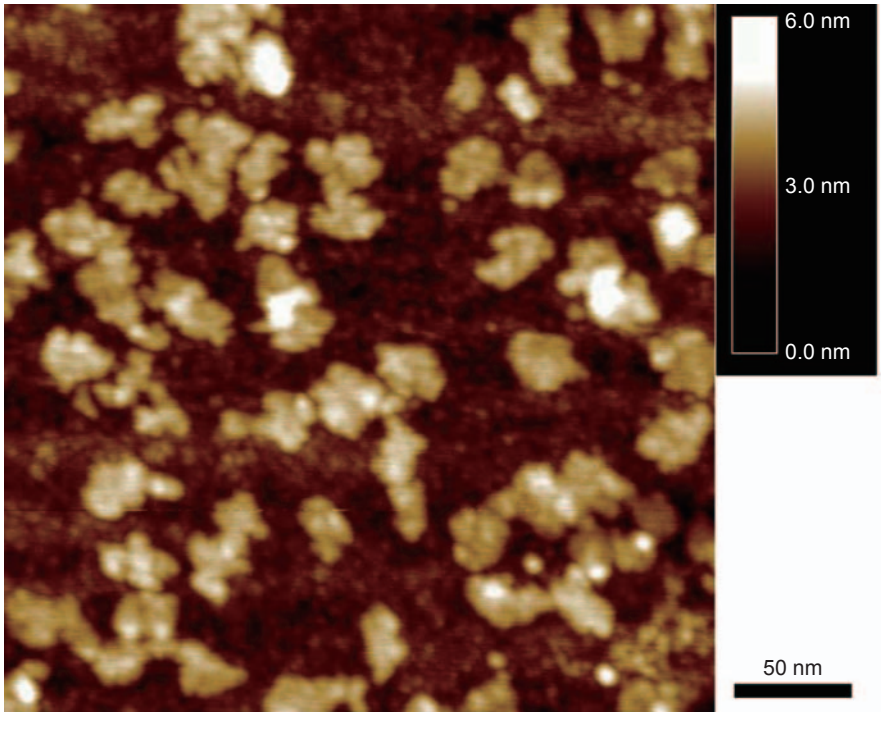

Figure S-3 AFM image of F23 after flattening at *Z*=6 nm. It clearly shows the existence of tiny domains in the NGO–PEG sheets. The sample was calcined at 350 °C for 10 min in order to remove PEG molecules

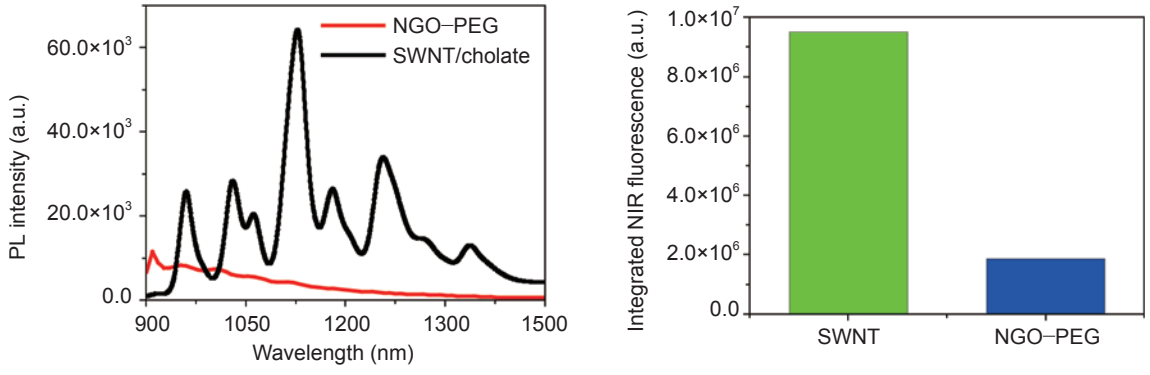

(a) (b)

Figure S-4 Comparison of photoluminescence of NGO–PEG and SWNT wrapped by cholate. (a) PL spectra of NGO–PEG and SWNT in the range 900–1500 nm under 785 nm excitation. (b) Integrated fluorescence ratio of SWNT compared with NGO–PEG. The data indicated the total integrated NIR fluorescence ratio of SWNT:NGO–PEG = 4.8:1 at 785 nm excitation. All these spectra were obtained after detector correction and normalized to absorbance at 785 nm

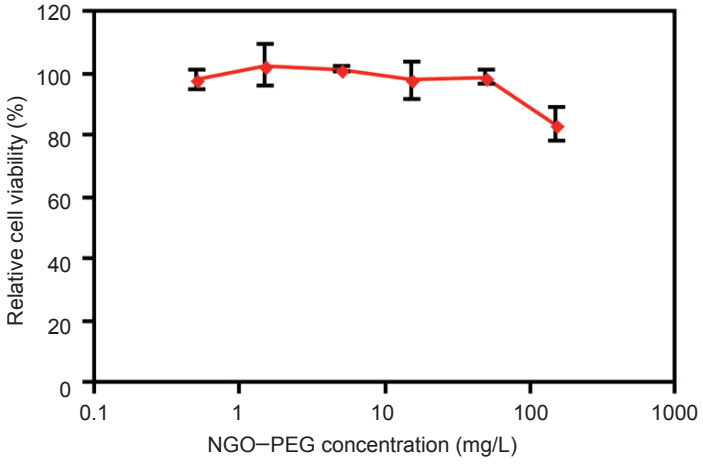

Figure S-5 Dosage-dependent cellular toxicity of NGO–PEG to Raji cells. Relative cell viabilities versus untreated control were plotted against NGO–PEG concentrations. No obvious toxicity was observed except a slight delay of cell growth at the highest NGO–PEG concentration (150 mg/L)

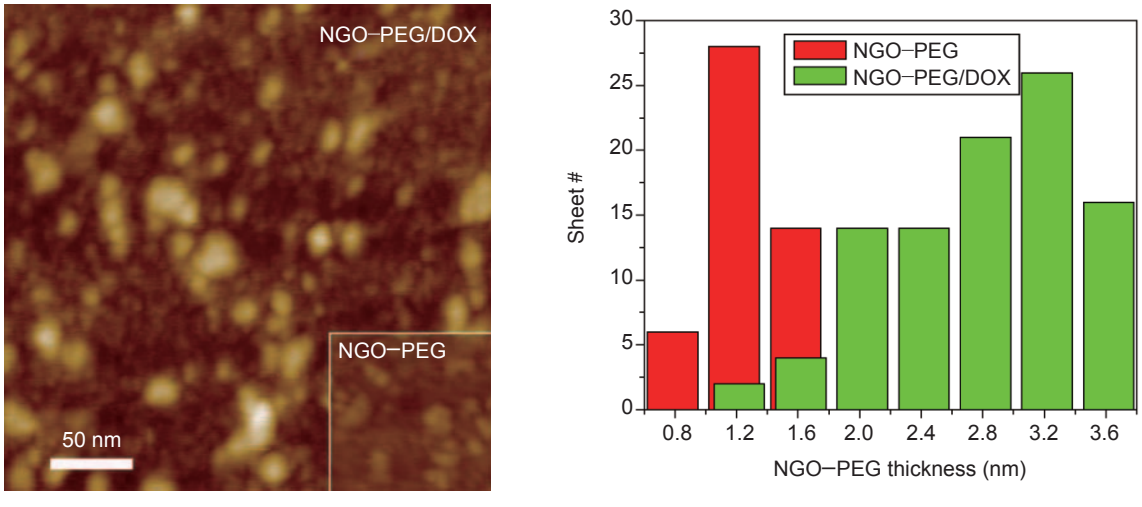

(a) (b)

Figure S-6 Comparison of thickness of NGO–PEG before and after DOX loading. (a) AFM of NGO–PEG after DOX loading, which showed obviously higher contrast than the original NGO–PEG shown in the inset. (b) Comparison of NGO–PEG layer thickness before (red columns) and after (green columns) DOX loading. An average thickness increase of ~2 nm was observed after DOX π-stacking